engineering proceedings

MDPI

Proceeding Paper

Virtual and Experimental Proof-of-Concept of a Delta Robot for Automated Packing of Automotive Metal Plates †

Ricardo J. M. Azevedo [1,2], César M. A. Vasques [1,2,*], Fernando A. V. Figueiredo [3,4] and Adélio M. S. Cavadas [1]

[1] Research Unit on Materials, Energy and Environment for Sustainability (proMetheus), School of Technology and Management, Polytechnic Institute of Viana do Castelo (IPVC), 4900-347 Viana do Castelo, Portugal; ricardoazevedo@ua.pt (R.J.M.A.); acavadas@estg.ipvc.pt (A.M.S.C.)
[2] Centre for Mechanical Technology and Automation (TEMA), Department of Mechanical Engineering, University of Aveiro, Campus Universitário de Santiago, 3810-193 Aveiro, Portugal
[3] Smile.Tech-Robótica, Rua de Bélgica 3213, 4400-055 Vila Nova de Gaia, Portugal; ff@smlt.pt
[4] Higher Institute of Entre Douro and Vouga (ISVOUGA), 4520-181 Santa Maria da Feira, Portugal
* Correspondence: cmavasques@ua.pt
† Presented at the 3rd International Electronic Conference on Machines and Applications, 12–14 May 2026; Available online: https://sciforum.net/event/IECMA2026.

Abstract

Manual handling and packing of thin metal plates remains a labour-intensive operation in the automotive manufacturing sector, frequently requiring multiple operators and resulting in limited productivity, reduced process repeatability, and ergonomic constraints. This paper presents a preliminary virtual and experimental proof-of-concept for the automation of such a packing task using a Delta robot, motivated by a representative industrial scenario involving automotive heat exchanger plates. The proposed study adopts an intentionally simplified problem formulation to support early-stage feasibility assessment and system design. In the considered scenario, nominal pickup and placement coordinates are predefined in the robot control program. The plates are manually aligned with marked pickup areas, while their actual physical poses are not measured or automatically corrected, allowing the study to focus on the robotic packing stage rather than on perception-based localization. A virtual robotic packing cell is developed using MATLAB-based simulation tools, with emphasis on functional sequence verification, workspace reachability, and end-effector integration. A set of preliminary feasibility indicators is considered, including reachability of the predefined positions, execution of the manipulation sequence, cycle time, end-effector behaviour, and correspondence between the planned and experimentally achieved layouts. The virtual model is used to support planning and preliminary analysis, while a simplified experimental demonstrator is implemented to verify the physical execution of the inclined-tray packing task using representative plate geometries. The experimental results provide a controlled functional feasibility baseline and identify part-presentation accuracy, sensing, calibration, and cycle-time reduction as the main requirements for further development.

Keywords: delta robot; robotic packing; virtual modelling; automotive manufacturing; end-effector design; experimental validation; proof-of-concept automation

Check for updates

Academic Editor: Marco Ceccarelli

Published: 18 August 2026

Copyright: © 2026 by the authors. Licensee MDPI, Basel, Switzerland. This article is an open access article distributed under the terms and conditions of the Creative Commons Attribution (CC BY) license.

1. Introduction

In the representative industrial case considered in this work, thin corrugated metallic plates used in automotive heat exchanger applications are manually handled and placed into trays through a repetitive, operator-dependent process. Although each plate has a low mass, the operation requires careful handling to avoid deformation, consistent positioning, and ordered tray placement. These requirements make the task suitable for robotic automation, while the repetitive manual process may also contribute to operator fatigue and exposure to work-related musculoskeletal disorder risk factors [1,2].

The evolution of industrial manufacturing relies heavily on the automation of repetitive material handling tasks to improve efficiency, productivity, and process repeatability. Among these tasks, high-speed pick-and-place operations are critical in high-throughput environments, where parts must be sorted, transferred, and positioned rapidly and accurately [3–5]. While recent Industry 5.0 developments increasingly rely on the integration of robotic manipulation with computer vision to enable adaptive and perception-driven automation [6], the present study intentionally considers a simplified scenario with predefined pickup and placement positions in order to assess the feasibility of the proposed robotic packing concept before introducing perception-related complexity.

To address these demands, Delta robots, originally introduced by Clavel as a parallel robotic architecture for the movement and positioning of an element in space, have become a reference solution for high-speed manipulation tasks [7,8]. By locating the main actuators on the fixed base, their structure significantly reduces moving mass, enabling high accelerations and operational speeds while maintaining high structural rigidity [9,10]. Recent studies also demonstrate that cost-effective platforms, such as the Delta Óscar robot used in this work, can achieve kinematic performance levels compatible with demanding high-speed manipulation tasks [11].

However, the physical deployment of parallel manipulators requires preliminary validation. Virtual commissioning has been widely used to support the validation of automated manufacturing systems before physical implementation, reducing development risks and commissioning effort [12,13]. Multibody simulation tools, such as Simscape Multibody, allow the modelling and simulation of three-dimensional mechanical systems and robotic mechanisms in a virtual environment [14–16]. The main technical and operational elements of the considered problem and their translation into the robotic proof-of-concept are summarized in Figure 1.

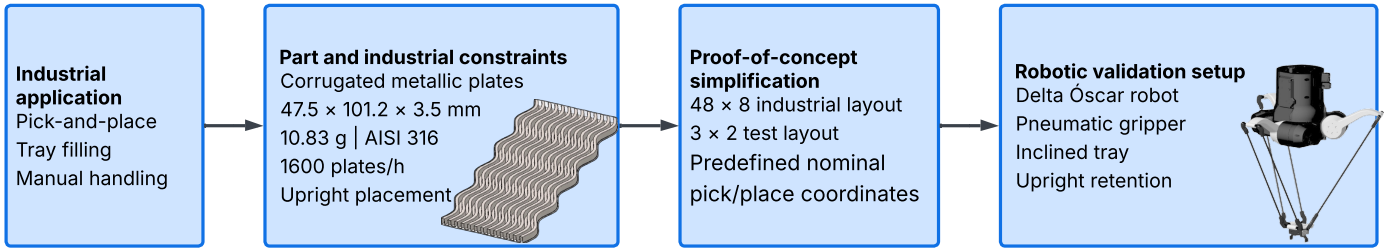


Figure 1. Overview of the industrial application, operational requirements, proof-of-concept simplification, and robotic validation setup.

From an industrial perspective, automation is justified by the need to reduce manual intervention, improve placement repeatability, and support a more stable production cadence. In the original production scenario, the plates are intended to be arranged in an ordered 48 × 8 tray layout while maintaining an upright orientation, with a target cadence of 1600 plates/h. For the present proof-of-concept, this requirement was simplified to a reduced 3 × 2 inclined-tray configuration. The inclined tray was adopted as a practical

solution to support upright retention of the plates after release, allowing the study to focus on the robotic packing stage while preserving the essential constraints of the industrial task: controlled grasping, transfer, release, final orientation, and retention inside the tray.

Based on the problem defined above, the objective of this work is to develop and assess a preliminary virtual and experimental proof-of-concept for the automated packing of thin corrugated metallic plates using a Delta robot.

Robot motion is generated using predefined nominal pickup and placement coordinates. In the experimental setup, the plates are manually aligned with marked pickup areas, while their actual poses and the tray alignment are not measured or automatically corrected. This simplification allows the study to focus on the robotic packing sequence, the custom end-effector, and the inclined-tray placement strategy.

The specific contribution of this study lies in the application-specific formulation and quantitative validation of a Delta robot-based solution for the upright packing of thin corrugated automotive plates. The proposed approach jointly addresses the application-specific requirements considered in this work by combining a profiled low-pressure pneumatic end-effector, an inclined-tray retention strategy, and repeated complete six-plate packing tests. The resulting feasibility baseline is quantified through workspace indicators, cycle time, tested stable motion conditions, success rate, and observed failure modes.

The remainder of this paper is organized as follows: Section 2 presents the system architecture and virtual modelling approach. Section 3 describes the end-effector design. Section 4 details the experimental implementation. Section 5 presents and discusses the results. Finally, Section 6 summarizes the main conclusions and future work.

2. System Architecture and Virtual Modelling

Before detailing the computational modeling process in MATLAB/Simulink and Simscape Multibody [17,18], it is essential to define the conceptual system architecture and the specific kinematic properties of the robotic platform that the virtual model aims to replicate.

2.1. Global System Architecture and the Delta Robot

The proposed robotic cell is organized into two functional levels: a computational level and a physical execution level. As shown in Figure 2, the computational level is used for trajectory generation and sequence planning, while the physical level includes the ReTRoC controller, the Delta Óscar robot, the pneumatic gripper, and the inclined-tray workspace. The ReTRoC controller manages the robot motion commands, serial communication, and digital outputs (DOs) used for gripper actuation. This organization allows representative manipulation cycles to be planned and evaluated virtually before being tested on the physical demonstrator.

The physical execution relies on the Óscar Delta robot, a cost-effective parallel manipulator [11]. Parallel kinematic machines (PKMs) feature closed-loop kinematic chains connecting a fixed base to a moving platform [9,10]. Unlike traditional serial manipulators, the Delta robot houses its three main active joints (actuators) on the fixed upper base.

Each actuator drives a rigid upper arm connected to a lower spatial parallelogram assembly. Instead of using conventional passive universal joints, the Óscar platform implements pairs of passive revolute joints arranged with mutually perpendicular axes at each end of the parallelogram links. This kinematically equivalent configuration provides the necessary degrees of freedom to ensure that the geometric constraints restrict the mobile end-effector platform to three purely translational degrees of freedom (3 DOF) along the X, Y, and Z axes, keeping it strictly parallel to the fixed base (Figure 3a).

https://doi.org/10.3390/engproc2026145013

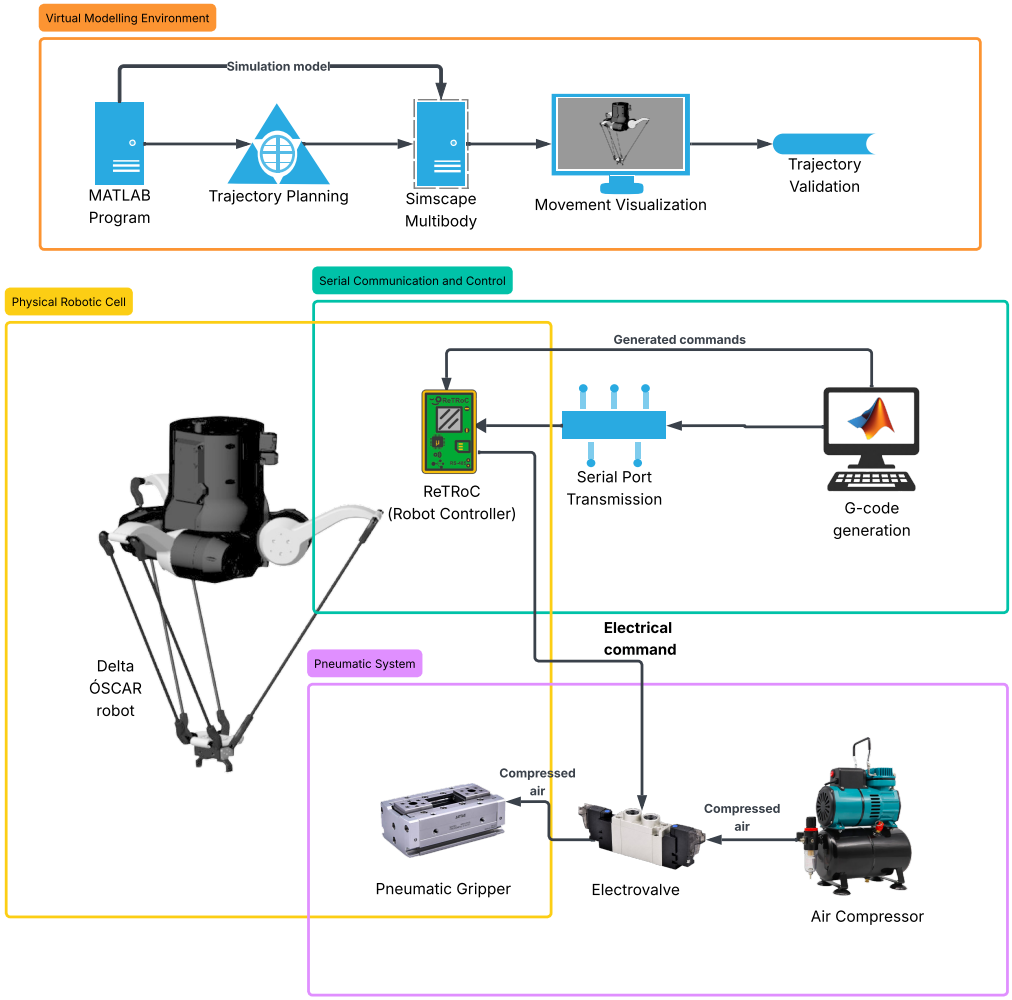


Figure 2. Global system architecture integrating the virtual planning environment, ReTRoC control unit, Delta Óscar robotic platform, pneumatic end-effector, solenoid valve, and air supply system [19–23].

To define the operational boundaries of the cell, the reachable volume of the Delta Óscar robot was estimated from its physical dimensions and joint operating limits. This evaluation followed general workspace-analysis principles for Delta robots, in which the reachable region is obtained from the geometric constraints imposed by the closed-loop parallel kinematic chains [24].

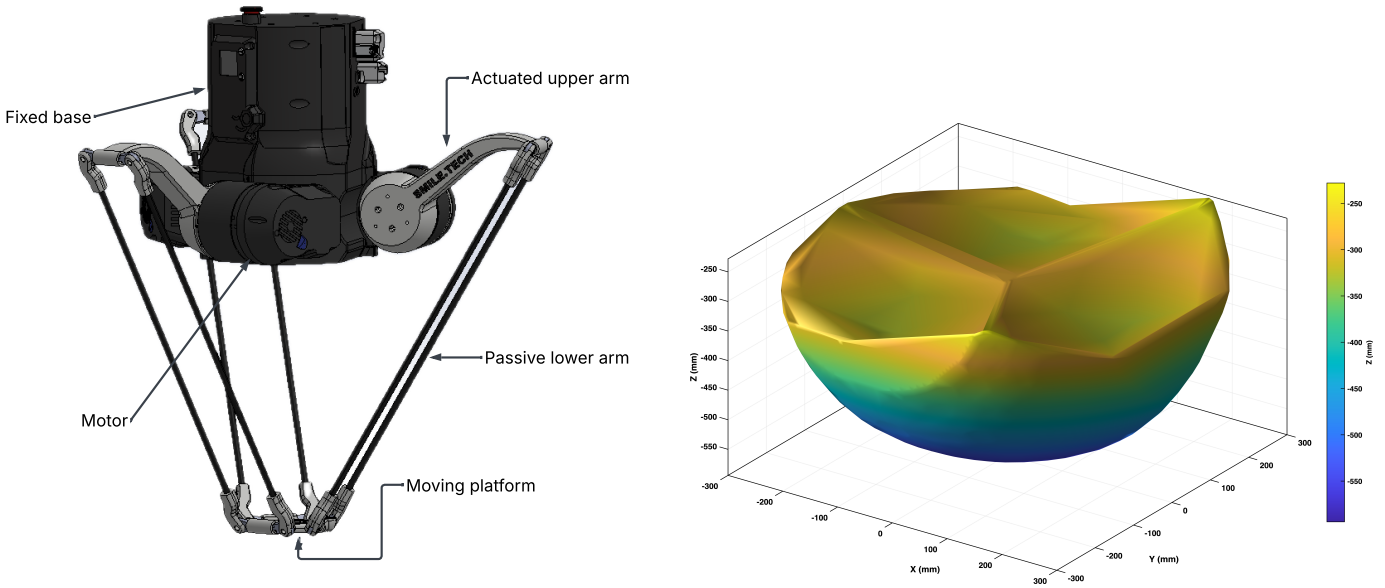
The workspace was estimated by evaluating a uniform Cartesian grid and retaining only the points for which real inverse-kinematic solutions existed for all three limbs within the imposed joint limits. The main calculation parameters are summarized in Table 1.

Table 1. Parameters used for the numerical workspace estimation.

Parameter	Value
Robot geometry	$d_{base} = 193.918$ mm, $d_{plat} = 60.62$ mm, $L = 163.898$ mm, $l = 448.0$ mm
Active-joint range	$[-45°, 80°]$
Cartesian search region	$x, y \in [-300, 300]$ mm; $z \in [-600, -200]$ mm
Grid resolution	6 mm; 683,467 candidate points
Reachability criterion	Real inverse-kinematic solutions for all three limbs within the joint limits

The workspace volume was approximated as $V \approx N_{\text{valid}}(6\,\text{mm})^3$, while the maximum horizontal diameter was calculated as $2\max\sqrt{x^2+y^2}$ and the vertical stroke as $z_{\max} - z_{\min}$.

The resulting reachable region did not correspond to a simple cylindrical volume, but to a downward-oriented dome-like workspace with a slightly concave upper profile, as shown in Figure 3b. The estimated workspace volume was 52.50 dm^3, with a maximum horizontal diameter of 712 mm and a vertical stroke of 366 mm, covering the main region required for the representative pick-and-place trajectory and the target tray positions considered in the proof-of-concept.



(**a**) (**b**)

Figure 3. Robotic platform analysis: (**a**) 3D CAD schematic highlighting the structural arms and perpendicular revolute joint architecture; (**b**) simulated reachable workspace of the Delta Óscar robot, with an approximate volume of 52.50 dm^3.

2.2. Simscape Multibody Implementation

The virtual modelling process was developed using MATLAB/Simulink and Simscape Multibody (R2025b), adapting established simulation methodologies for parallel kinematic mechanisms [17,18]. Multibody simulation provides an effective framework for analysing robotic kinematics and dynamics while supporting virtual validation prior to physical implementation [25]. To prevent constraint inconsistencies typical of automated CAD imports in closed-loop chains, the kinematic structure was explicitly defined, utilizing the CAD files exclusively as geometric and inertial references.

The resulting Simscape Multibody model was organized hierarchically, as shown in Figure 4. At the top level, the model includes the fixed base, the three equivalent kinematic limb subsystems, the moving platform, the gripper, the workpiece plate, the contact model, and the output sensing blocks. This organization allowed the structural model of the Delta robot to be separated from the gripper–plate interaction and from the sensor outputs, making the virtual environment easier to interpret and modify.

Each limb subsystem includes the corresponding upper- and lower-arm assemblies connected through active revolute joints and passive joint/link elements to preserve the geometric constraints of the parallel manipulator. The gripper and manipulated plate were integrated using Spatial Contact Force blocks, enabling the simulation of the physical interactions occurring during approach, grasping, transfer, and placement.

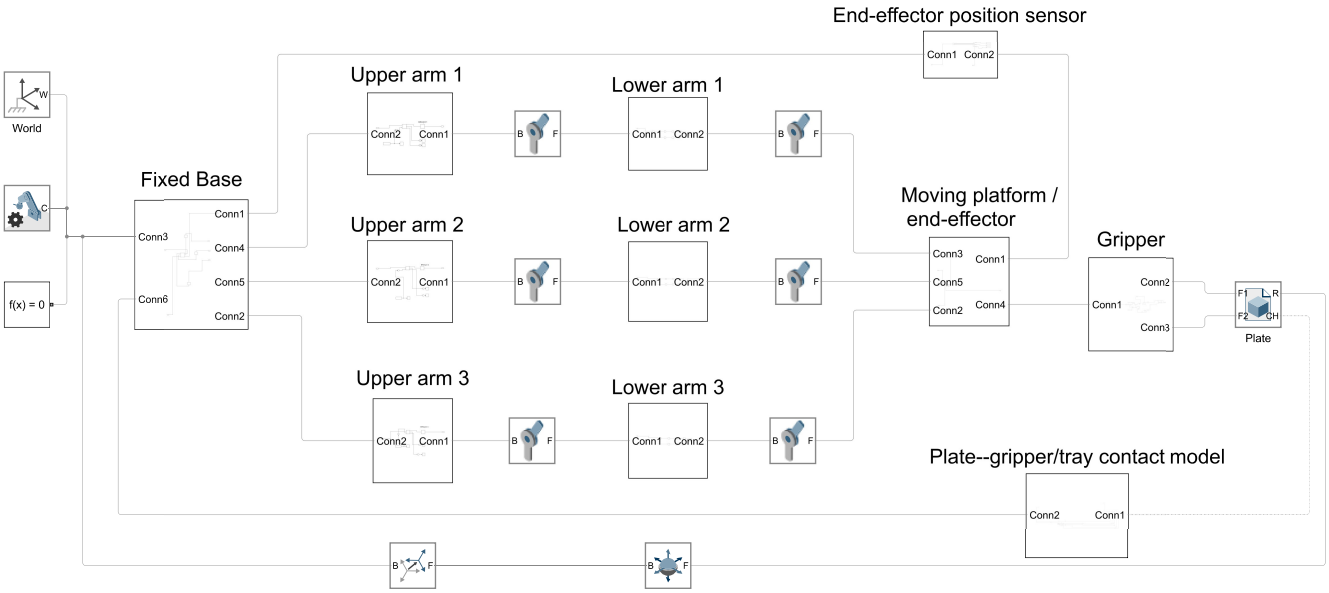


Figure 4. Top-level organization of the Simscape Multibody model used for the virtual Delta robot cell.

Driven by a trajectory generation module using continuous interpolation profiles, this simulated environment enables a rapid preliminary evaluation of workspace accessibility, joint motion consistency, and collision-aware path planning prior to physical hardware deployment.

3. End-Effector Design

The end-effector was developed as a task-oriented component to provide a stable mechanical interface between the pneumatic actuator and the corrugated plate during proof-of-concept validation. The objective was not to achieve full geometric optimization, but rather to obtain a practical and lightweight solution enabling repeatable grasping, transfer, and release of representative plates with minimal added mass on the Delta robot moving platform.

The primary design driver was to prevent any localized part deformation, since the thin corrugated plates are highly sensitive to contact pressure. Consequently, the contact strategy was selected to favor geometric engagement rather than high clamping forces. The inner profile of the fingers was specifically shaped to follow the overall plate geometry, providing a seating surface that constrains the part laterally during transfer while keeping the contact pressure low. The operating pressure of 1.5 bar was selected experimentally as the minimum value providing reliable grasping without inducing visible deformation of the corrugations during preliminary trials.

The remaining structural design strategies focused on mass reduction and system modularity. The end-effector body and contact fingers were manufactured by fused deposition modelling (FDM, material extrusion) using polylactic acid (PLA), enabling rapid design iterations, low manufacturing cost, and straightforward fabrication of customized components. The body was hollowed to reduce the moving mass attached to the Delta platform while maintaining sufficient stiffness for the low payload considered in this work. The contact fingers were designed as replaceable components, fixed to the main body through a bolted interface, facilitating future adaptation to different plate geometries.

Although conventional PLA was employed in the present prototype, future developments may exploit conductive carbon-filled PLA materials exhibiting piezoresistive behaviour to integrate distributed force or deformation sensing directly into the end-effector structure, potentially enhancing grasp monitoring without requiring additional external sensors [26]. Furthermore, for applications involving higher payloads or more de-

manding operating conditions, metallic additive manufacturing technologies, such as laser powder bed fusion (LPBF), could be employed to produce end-effector components with enhanced mechanical performance, stiffness, and structural robustness while preserving the geometric flexibility offered by additive manufacturing [27].

To clearly summarize the engineering methodology, these design requirements, the corresponding adopted strategies, and the resulting physical specifications are systematically mapped in the conceptual framework shown in Figure 5.

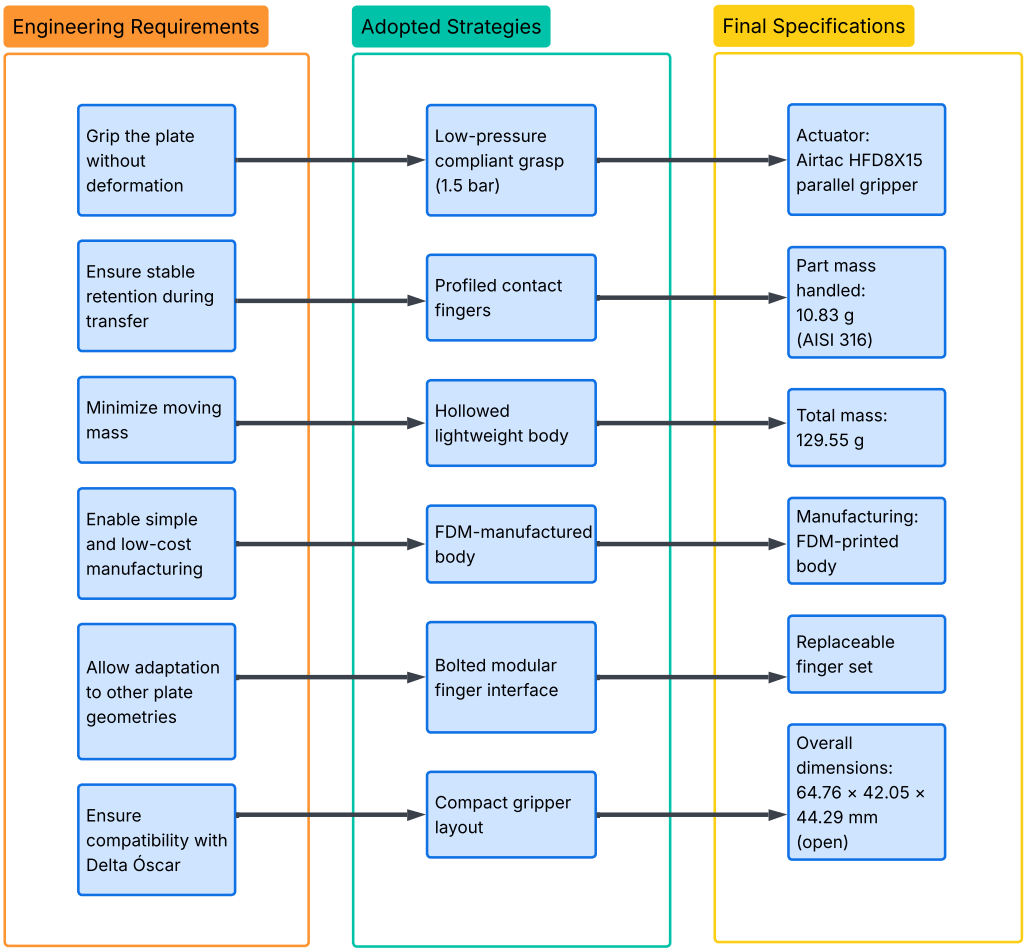
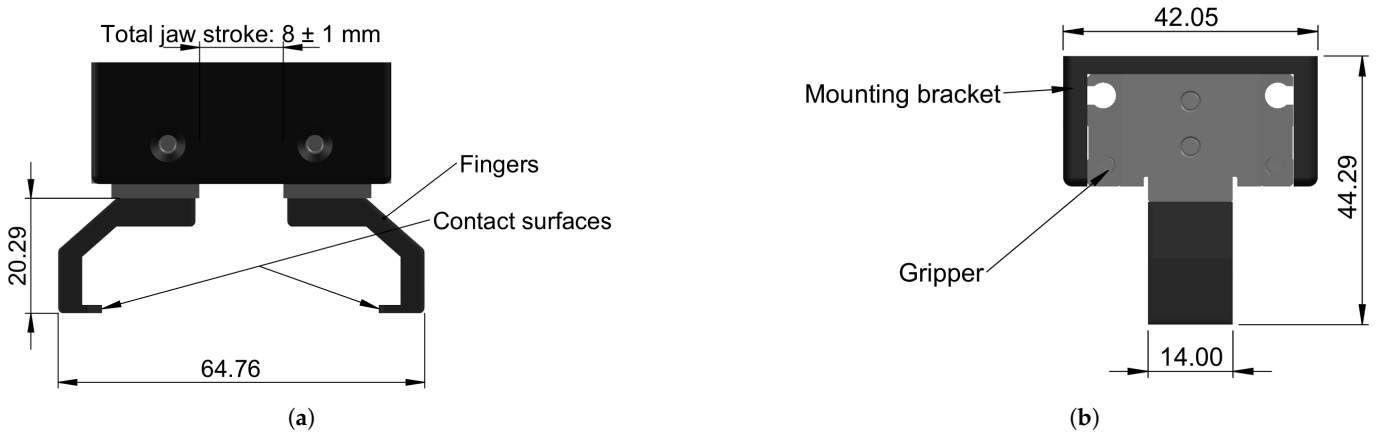


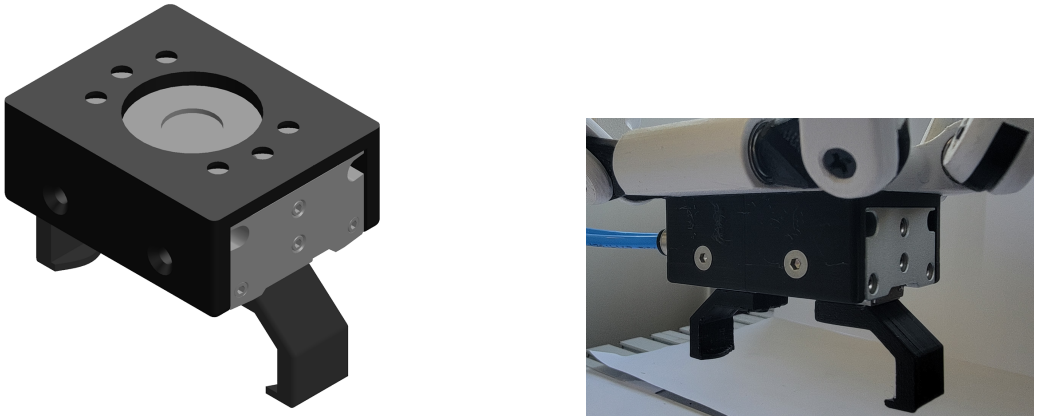
Figure 5. Design rationale framework mapping the main requirements to the adopted strategies and final hardware specifications of the custom end-effector.

The proposed end-effector is application-specific; changes in plate geometry, thickness, or surface condition may require adjustments to the finger profile. For this reason, the fingers were designed as replaceable components fixed to the main body through a bolted interface. The annotated dimensioned views in Figure 6 define the main external dimensions of the assembly, the useful jaw stroke, the mounting bracket, and the finger spacing in the open state. Figure 7 shows the CAD configuration and the integrated prototype mounted on the robot.



(**a**) (**b**)

Figure 6. Annotated dimensioned views of the custom pneumatic end-effector: (**a**) front view with the fingers in the open state and useful jaw stroke [21]; (**b**) right-side view identifying the mounting bracket and gripper body.



(**a**) (**b**)

Figure 7. Custom pneumatic end-effector implementation: (**a**) CAD isometric view showing the c integrated with the FDM-printed body; (**b**) integrated prototype mounted on the Delta Óscar robot during a manipulation test.

4. Experimental Implementation

The experimental implementation was used to assess the physical execution of the inclined-tray packing sequence under controlled laboratory conditions. Since the global cell architecture was introduced in Section 2, this section focuses only on the experimental configuration, operating parameters, and test procedure.

The test was performed with the Delta Óscar robot (Smile.Tech Robótica, Vila Nova de Gaia, Portugal) equipped with the custom pneumatic end-effector described in Section 3. The end-effector integrates an Airtac HFD8X15 (AirTAC International Group, Taipei City, Taiwan) parallel pneumatic gripper [21] actuated by an Airtac 7V0520-M5 dual-coil solenoid valve (AirTAC International Group, Taipei City, Taiwan) [22]. Compressed air was supplied by a VEVOR TC-20B compressor (Shanghaimuxinmuyeyouxiangongsi, Shanghai, China) [23]. The valve was connected to the robot controller through digital output channels, allowing gripper actuation to be synchronized with the programmed robot motion.

Figure 8 shows the experimental packing area used in the test, identifying the main functional elements of the setup. The experimental configuration consisted of an inclined tray designed to receive six representative corrugated metallic plates in an upright orientation, following a 3 × 2 target layout. Before the final assessment, the robot velocity, vertical clearances, gripper actuation timing, pneumatic pressure, and placement height

were adjusted empirically to improve grasping, transfer, and release reliability. The main hardware components and baseline operating conditions are summarized in Table 2.

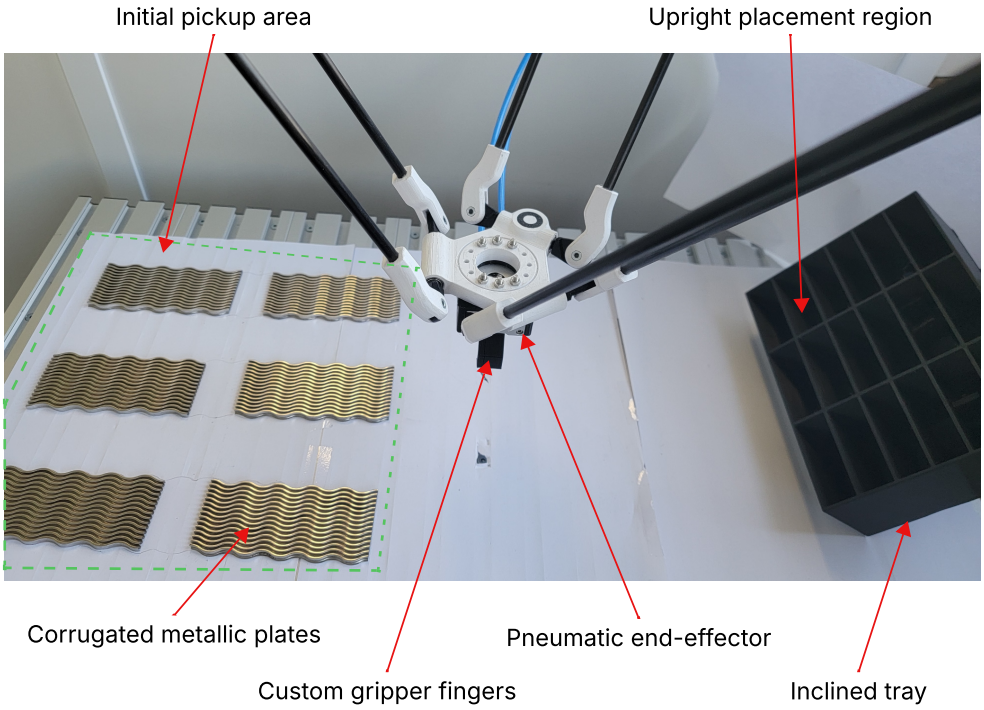


Figure 8. Detail of the experimental packing area used in the inclined-tray test, identifying the pneumatic end-effector, pickup area, representative corrugated plates, inclined tray, and upright placement region.

Table 2. Main components and baseline operating conditions used in the inclined-tray packing test.

Item	Description/Value
Robot platform	Delta Óscar
Pneumatic gripper	Airtac HFD8X15 [21]
Solenoid valve	Airtac 7V0520-M5 [22]
Air supply	VEVOR TC-20B compressor [23]
Working pressure	1.5 bar
Motion programming	MATLAB-generated G-code sequence
Gripper actuation	Robot controller digital outputs
Baseline programmed velocity	150 mm/s
Manipulated parts	Corrugated metallic plates
Number of plates	6
Target layout	3 × 2 inclined tray
Final plate orientation	Upright orientation

For each plate, the MATLAB-generated G-code sequence consisted of approach, vertical descent, gripper closing, lifting, transfer to the inclined tray, descent to the assigned placement position, gripper opening, and return to a safe height.

Repeated-Test Protocol and Evaluation Criteria

After the preliminary motion-parameter assessment, 25 complete six-plate packing sequences were performed using the selected stable configuration. Before each sequence, the plates were manually returned to their nominal pickup areas using markings on the worktable. The same predefined pickup and placement coordinates were used in all

repetitions, without vision-based pose measurement or precision positioning fixtures for the plates or tray.

A sequence was considered successful when all six plates were correctly arranged and retained in the intended upright 3×2 layout without manual correction or robot motion interruption. A sequence was considered failed when at least one plate was not correctly arranged in the tray at the end of the cycle.

5. Results and Discussion

The results were evaluated at two levels. First, the virtual model was used to verify a representative single-plate pick-and-place cycle in the Simscape Multibody environment, with gravity and contact forces enabled. Second, the experimental setup was used to assess the physical execution of the inclined-tray packing task with six representative corrugated plates.

Although the target packing layout corresponds to a 3×2 arrangement, the virtual validation presented in this work focused on one complete manipulation cycle. This approach was adopted to verify the functional integration between the Delta robot, the gripper, the handled plate, and the inclined tray before extending the virtual model to the complete multi-plate sequence.

Gravity was enabled during the simulation, and contact force elements were used to model the interaction between the gripper fingers and the plate, as well as between the plate and the tray. The contact model was used for functional verification of the manipulation sequence and was not calibrated as a detailed dynamic contact model.

5.1. Virtual Single-Plate Pick-And-Place Cycle

The virtual sequence included the main stages of the operation: approach to the plate, pickup, gripper closing, lifting, transfer to the tray, placement, horizontal insertion, gripper opening, and retraction. Contact force elements were defined between the gripper fingers and the plate, as well as between the plate and the tray, in order to reproduce the main physical interactions during the placement operation. Figure 9 shows the main stages of the representative single-plate pick-and-place cycle in the Simscape Multibody environment.

Table 3 summarizes the main functional indicators obtained from the representative virtual cycle.

Table 3. Summary of the representative virtual pick-and-place cycle.

Indicator	Result
Evaluated sequence	Single pick-and-place cycle
Number of plates dynamically evaluated	1
Target packing layout	3×2
Gravity	Enabled
Finger–plate contact force	Enabled
Plate–tray contact force	Enabled
Gripper motion	Synchronized with robot motion
Useful cycle time	19.0 s

The commanded motion was defined in joint space and applied to the three active revolute joints of the virtual Delta robot. Figure 10 shows the corresponding joint position, velocity, and acceleration command profiles, together with the gripper opening command used to synchronize grasping and release during the representative pick-and-place cycle. The gripper signal is represented as a relative opening command, where 0 mm corresponds to the closed state.

In addition to the commanded joint profiles, the simulated Cartesian response of the end-effector was obtained from the Transform Sensor placed at the moving platform. Figure 11 presents the corresponding displacement, velocity, and acceleration components during the same representative cycle. The Cartesian displacement is represented relative to the initial pose of the useful cycle in order to highlight the effective motion performed during the pick-and-place operation.

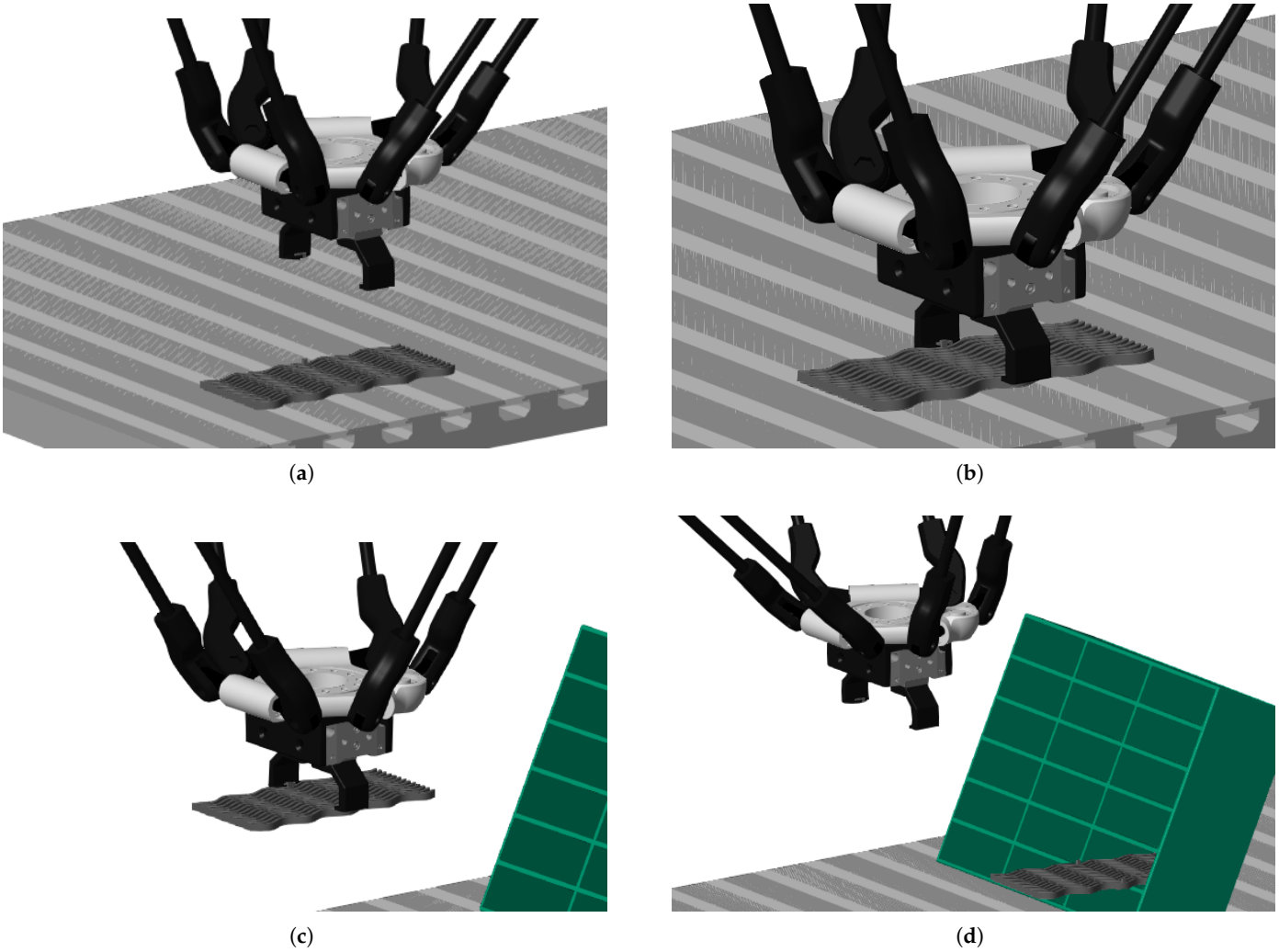


Figure 9. Virtual execution of the representative single-plate pick-and-place cycle with gravity and contact forces enabled: (**a**) approach to the plate; (**b**) pickup/grasping stage; (**c**) transfer towards the inclined tray; (**d**) plate after placement in the tray.

The useful cycle time was 19.0 s, corresponding to the interval from the motion towards the pickup position until the retraction after the plate release. The results show that the virtual model can reproduce a complete single-plate handling operation, including grasping, transfer, contact-enabled placement, and release inside the inclined tray. However, the complete 3×2 packing sequence was not fully validated at this stage, since its extension requires further refinement of the inverse kinematic implementation and frame correspondence between the analytical model and the Simscape Multibody model.

5.2. Experimental Packing Results

The experimental tests were performed using the inclined-tray configuration described in Section 4. The objective was to transfer six corrugated metallic plates from the pickup area to the tray and obtain an upright 3×2 final layout. Figure 12 compares the initial

pickup arrangement of the corrugated plates with the final upright arrangement obtained inside the inclined tray after the experimental sequence.

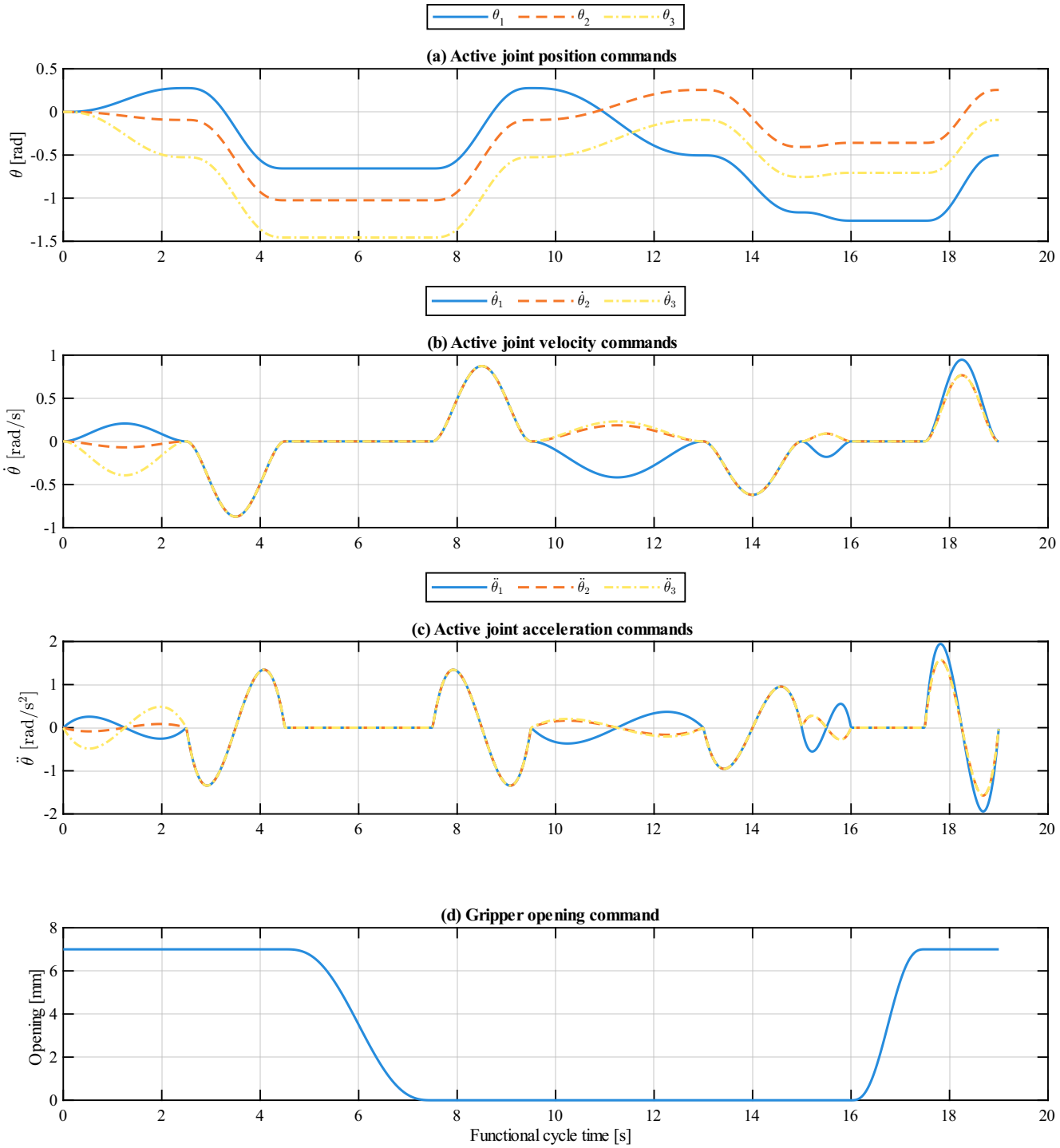


Figure 10. Joint-space command profiles used in the representative virtual pick-and-place cycle: (**a**) active joint position commands; (**b**) active joint velocity commands; (**c**) active joint acceleration commands; (**d**) gripper opening command.

Different programmed velocities, accelerations, and jerk values were tested to evaluate their influence on cycle time and manipulation reliability. The tested conditions are summarized in Table 4.

https://doi.org/10.3390/engproc2026145013

Configuration 4 was selected as the fastest tested condition that maintained stable grasping, transfer, release, and upright retention of the plates. The main performance indicators obtained with this configuration are presented in Table 5.

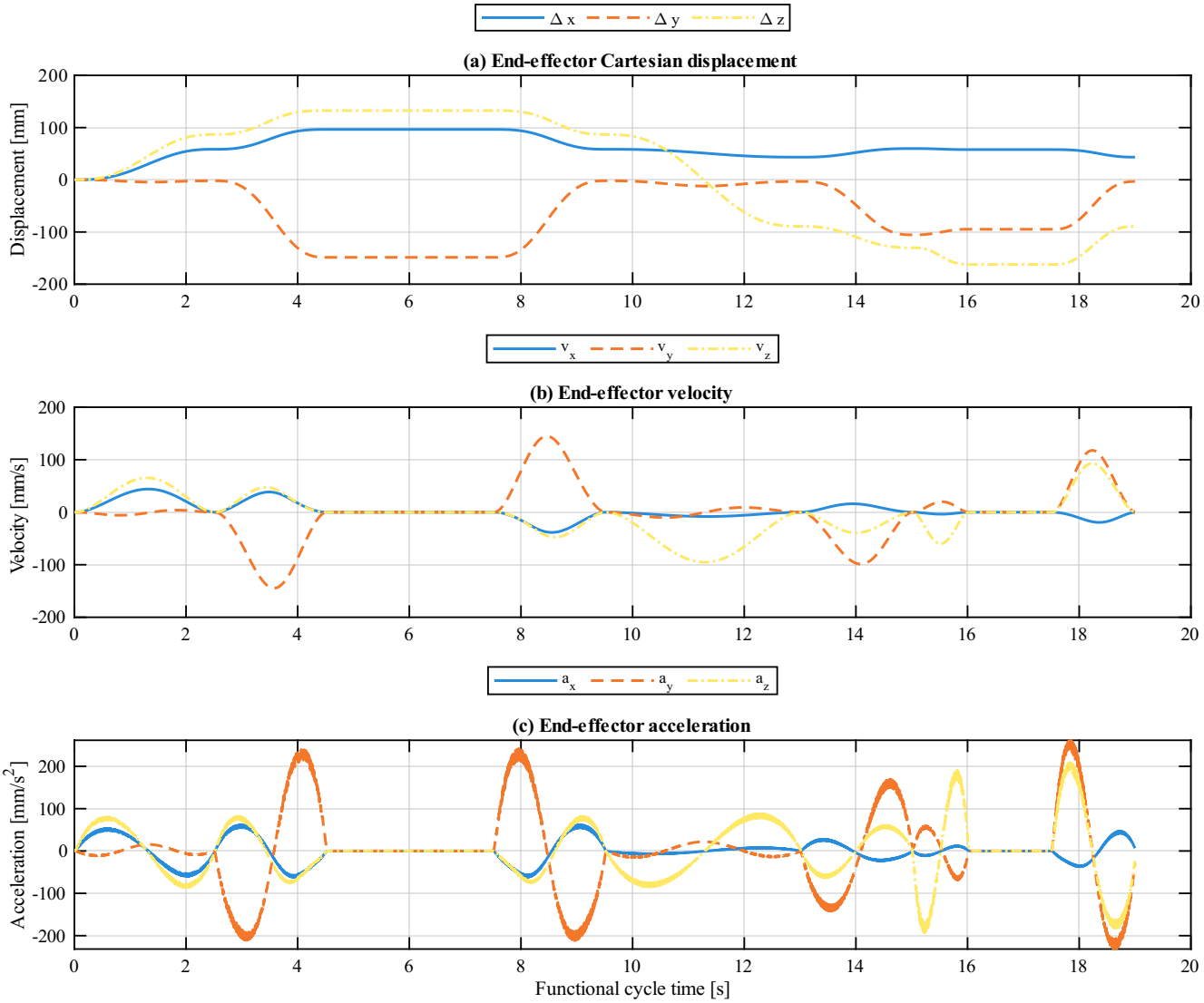
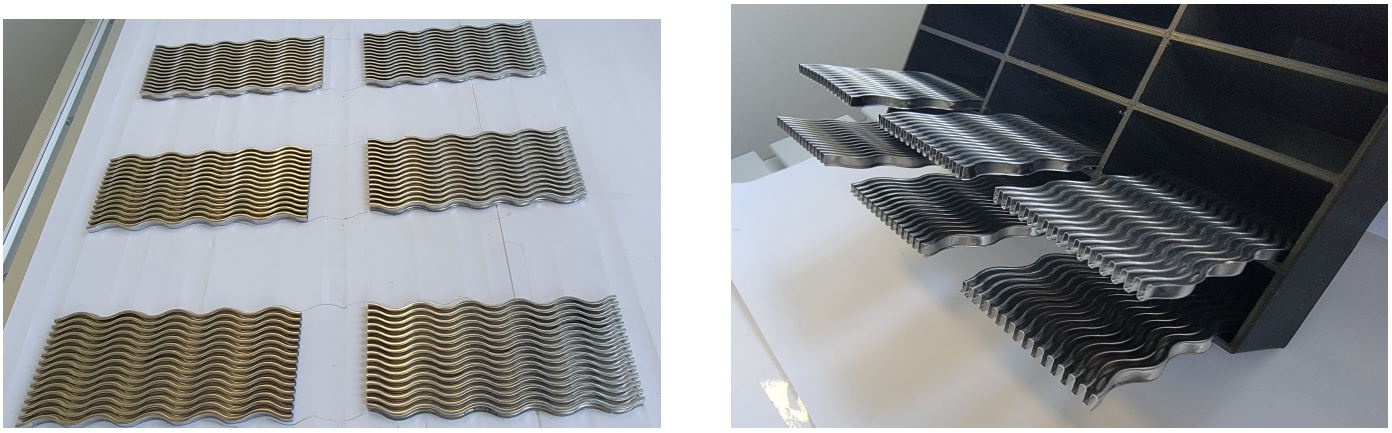


Figure 11. Simulated Cartesian response of the end-effector during the representative virtual pick-and-place cycle: (**a**) Cartesian displacement relative to the initial pose; (**b**) Cartesian velocity components; (**c**) Cartesian acceleration components.

Table 4. Experimental results obtained for the tested motion configurations.

Configuration	Velocity [mm/s]	Acceleration [mm/s^2]	Jerk [mm/s^3]	Result	Time [s]	Observation
1	150	200	15,000	Success	58	Stable baseline condition
2	280	540	20,000	Success	44	Stable transfer and upright placement
3	350	800	23,000	Success	35	Stable manipulation with reduced cycle time
4	400	800	30,000	Success	33	Highest stable tested condition
5	400	1200	30,000	Failure	Interrupted	Motion fault; sequence interrupted

https://doi.org/10.3390/engproc2026145013



(**a**) (**b**)

Figure 12. Experimental inclined-tray packing result: (**a**) initial arrangement of the six corrugated plates; (**b**) final 3 × 2 arrangement after placement inside the inclined tray, with the plates retained in an upright orientation.

Table 5. Performance indicators for the selected inclined-tray packing sequence.

Indicator	Result
Number of plates manipulated per sequence	6
Target layout	3 × 2
Final layout achieved	Yes
Final plate orientation	Upright
Manual correction during successful sequences	No
Plate loss during successful sequences	No
Visible plate deformation	No
Selected programmed velocity	400 mm/s
Selected acceleration	800 mm/s^2
Selected jerk setting	30,000 mm/s^3
Total sequence time	33 s
Average time per plate	5.50 s/plate
Estimated cadence	655 plates/h
Repeated complete six-plate sequences	25
Successful sequences	22
Failed sequences	3
Success rate	88%
Observed failure mode	Incorrect plate placement following plate–tray contact

The average time per plate was computed from the total sequence time divided by the six manipulated plates. The estimated cadence was calculated as

$$C = \frac{3600}{t_p}, \tag{1}$$

where C is the estimated cadence in plates per hour and t_p is the average time per plate in seconds. For the selected configuration, the complete six-plate sequence required 33 s, corresponding to 5.50 s/plate and an estimated cadence of 655 plates/h.

The tested conditions show that increasing the programmed velocity and acceleration reduced the cycle time while maintaining stable manipulation up to 400 mm/s and 800 mm/s^2. For the same velocity, increasing the acceleration to 1200 mm/s^2 triggered a motion fault and interrupted the sequence. Therefore, the 400 mm/s and 800 mm/s^2 condition was selected as the highest stable condition achieved in the current proof-of-concept setup. All 25 repeated sequences were performed using Configuration 4; the

interrupted Configuration 5 trial was part of the preliminary parameter assessment and was not included in these repetitions.

In the three failed sequences, at least one plate was incorrectly positioned inside the tray following plate–tray contact during placement. Since the actual plate positions and tray alignment were not measured, the failures could not be attributed to a single confirmed cause. They may have resulted from deviations in manual plate positioning, tray alignment, or a combination of both.

The achieved cadence remains below the target industrial requirement of 1600 plates/h, corresponding to approximately 41% of the target value. This result confirms the functional feasibility of the robotic packing strategy, but also shows that additional cycle-time reduction is required for industrial deployment.

Meeting the industrial target with a single robot would require reducing the cycle time from 5.50 to 2.25 s/plate, corresponding to a 59.1% reduction. This is unlikely to be achieved by increasing velocity alone, since Configuration 4 was the fastest stable condition tested and a higher acceleration caused a motion fault. Two equivalent stations would produce approximately 1310 plates/h at the current performance, but would meet the target with a moderate reduction to 4.50 s/plate per station. This could be pursued through trajectory and pneumatic-cycle optimization, reduced non-productive motion or improved positioning.

6. Conclusions

This work presented a virtual and experimental proof-of-concept for the automated packing of representative corrugated metallic plates using a Delta robot. The study focused on a controlled open-loop scenario using predefined nominal pickup and placement coordinates, allowing the analysis to concentrate on end-effector design, system integration, virtual single-cycle verification, and experimental packing tests.

The virtual model was used to verify a representative single-plate pick-and-place cycle with gravity and contact forces enabled. This test confirmed the functional integration of the robot motion, gripper actuation, plate handling, and contact-enabled placement inside the inclined tray. The complete 3×2 sequence was not fully validated in the virtual environment at this stage.

Experimentally, the developed setup demonstrated the physical execution of the six-plate packing concept. The selected motion condition placed six plates in 33 s, corresponding to 5.50 s/plate and an estimated cadence of 655 plates/h. In 25 repeated complete six-plate sequences, 22 were successfully completed, resulting in an 88% success rate. In the three failed sequences, at least one plate was incorrectly positioned following plate–tray contact during placement. Because the actual plate positions and tray alignment were not measured, a single confirmed cause could not be isolated.

Although the achieved cadence corresponds to approximately 41% of the target industrial requirement of 1600 plates/h, the results demonstrate the functional feasibility of the proposed robotic packing approach under controlled laboratory conditions. The main limitations are the open-loop operation using predefined nominal coordinates, the absence of automatic pose measurement and correction, the need for improved virtual-to-physical calibration, and the lack of quantitative placement accuracy and pose-repeatability measurements.

Future work should focus on vision-based plate pose estimation, improved mechanical referencing of the pickup area and tray, robot and trajectory calibration, refinement of the virtual contact model, and cycle-time reduction. Parallel packing stations should also be evaluated if optimization of a single cell remains insufficient to meet the required industrial cadence.

https://doi.org/10.3390/engproc2026145013

Author Contributions: Conceptualization, R.J.M.A., C.M.A.V. and F.A.V.F.; methodology, R.J.M.A., C.M.A.V. and F.A.V.F.; software, R.J.M.A.; validation, R.J.M.A., C.M.A.V., F.A.V.F. and A.M.S.C.; formal analysis, R.J.M.A., C.M.A.V. and F.A.V.F.; investigation, R.J.M.A. and C.M.A.V.; resources, C.M.A.V. and A.M.S.C.; writing—original draft preparation, R.J.M.A.; writing—review and editing, R.J.M.A. and C.M.A.V.; funding acquisition, C.M.A.V. and A.M.S.C. All authors have read and agreed to the published version of the manuscript.

Funding: This research received no external funding.

Data Availability Statement: The original contributions presented in this study are included in the article. Further inquiries can be directed to the corresponding author.

Acknowledgments: The authors gratefully acknowledge the funding provided by the Foundation for Science and Technology (FCT), Portugal, through the Research Unit in Materials, Energy and Environment for Sustainability (proMetheus) at the Polytechnic Institute of Viana do Castelo (IPVC), Viana do Castelo, Portugal, and through the Centre for Mechanical Technology and Automation (TEMA) at the University of Aveiro, Portugal. Additional support was provided within the scope of the project "Agenda DRIVOLUTION: Transition to the Factory of the Future" (project no. C632394276-0046698; operation code 02/C05-i01.02/2022.PC644913740-00000022), under the Agendas/Mobilizing Alliances for Reindustrialization initiative of the Portuguese Recovery and Resilience Plan (PRR).

Conflicts of Interest: Fernando A. V. Figueiredo is affiliated with Smile.Tech-Robótica, manufacturer of the Delta Óscar robot used in this study. The remaining authors declare no conflicts of interest.

Abbreviations

The following abbreviations are used in this manuscript:

CAD	Computer-aided design
DO	Digital output
DOF	Degree of freedom
FDM	Fused deposition modelling
PKM	Parallel kinematic machine
PLA	Polylactic acid
ReTRoC	Real Time Robot Controller
VC	Virtual commissioning
WMSD	Work-related musculoskeletal disorder

References

1. Punnett, L.; Wegman, D.H. Work-Related Musculoskeletal Disorders: The Epidemiologic Evidence and the Debate. *J. Electromyogr. Kinesiol.* **2004**, *14*, 13–23. [CrossRef] [PubMed]
2. da Costa, B.R.; Vieira, E.R. Risk Factors for Work-Related Musculoskeletal Disorders: A Systematic Review of Recent Longitudinal Studies. *Am. J. Ind. Med.* **2010**, *53*, 285–323. [CrossRef] [PubMed]
3. Xie, Z.; Wu, P.; Ren, P. A Comparative Study on the Pick-and-Place Trajectories for a Delta Robot. In Proceedings of the ASME 2016 International Design Engineering Technical Conferences and Computers and Information in Engineering Conference, Charlotte, NC, USA, 21–24 August 2016. [CrossRef]
4. Su, T.; Cheng, L.; Wang, Y.; Liang, X.; Zheng, J.; Zhang, H. Time-Optimal Trajectory Planning for Delta Robot Based on Quintic Pythagorean-Hodograph Curves. *IEEE Access* **2018**, *6*, 28531–28544. [CrossRef]
5. Kozman, P.; Hilmy, M.; Makin, O.; Hammad, Y.; Hagag, E.E.; Ahmed, O.; Ilias, G.; Awad, M.I.; Maged, S.A. 4 DOFs High-Speed Pick and Place Delta Robot. In Proceedings of the 16th International Conference on Computer Engineering and Systems (ICCES), Cairo, Egypt, 15–16 December 2021. [CrossRef]
6. Varolia, H.; Vasques, C.M.A.; Cavadas, A.M.S. Computer Vision for Collaborative Robots in Industry 5.0: A Survey of Techniques, Gaps, and Future Directions. *Eng. Proc.* **2026**, *124*, 99. [CrossRef]
7. Clavel, R. DELTA, a Fast Robot with Parallel Geometry. In Proceedings of the 18th International Symposium on Industrial Robots, Lausanne, Switzerland, 26–28 April 1988; pp. 91–100.
8. Clavel, R. Device for the Movement and Positioning of an Element in Space. U.S. Patent 4,976,582, 11 December 1990.

9. Merlet, J.P.; Gosselin, C. Parallel Mechanisms and Robots. In *Springer Handbook of Robotics*, 2nd ed.; Siciliano, B.; Khatib, O., Eds.; Springer: Berlin, Germany, 2016; Chapter 12.
10. Russo, M.; Zhang, D.; Liu, X.J.; Xie, Z. A Review of Parallel Kinematic Machine Tools: Design, Modeling, and Applications. *Int. J. Mach. Tools Manuf.* **2024**, *196*, 104118. [CrossRef]
11. Vasques, C.M.A.; Figueiredo, F.A.V. The 3D-Printed Low-Cost Delta Robot Óscar: Technology Overview and Benchmarking. *Eng. Proc.* **2021**, *11*, 12. [CrossRef]
12. Lee, C.G.; Park, S.C. Survey on the Virtual Commissioning of Manufacturing Systems. *J. Comput. Des. Eng.* **2014**, *1*, 213–222. [CrossRef]
13. Lechler, T.; Fischer, E.; Metzner, M.; Mayr, A.; Franke, J. Virtual Commissioning—Scientific Review and Exploratory Use Cases in Advanced Production Systems. *Procedia CIRP* **2019**, *81*, 1125–1130. [CrossRef]
14. Pozzi, M.; Achilli, G.M.; Valigi, M.C.; Malvezzi, M. Modeling and Simulation of Robotic Grasping in Simulink Through Simscape Multibody. *Front. Robot. AI* **2022**, *9*, 873558. [CrossRef] [PubMed]
15. Boschetti, G.; Sinico, T. Designing Digital Twins of Robots Using Simscape Multibody. *Robotics* **2024**, *13*, 62. [CrossRef]
16. MathWorks. *Simscape Multibody User's Guide*; The MathWorks, Inc.: Natick, MA, USA, 2026; Version 26.1 (R2026a), revised March 2026. Available online: https://www.mathworks.com/help/pdf_doc/sm/sm_ug.pdf (accessed on 22 April 2026).
17. Walica, D.; Noskievič, P. Multibody Simulation Model as Part of Digital Twin Architecture. *IEEE Access* **2024**, *12*, 248–261. [CrossRef]
18. MathWorks. Pick and Place Robot Using Forward and Inverse Kinematics. Simscape Multibody Example. Available online: https://www.mathworks.com/help/sm/ug/pick-and-place-robot.html (accessed on 1 April 2026).
19. MathWorks. MATLAB Brand Guide: Logos and Icons. Online, 2026. Available online: https://www.mathworks.com (accessed on 20 May 2026).
20. Smile.Tech Robótica. ReTRoC—Real Time Robot Controller. Online Product Documentation, 2026. Available online: https://smlt.pt/strp-smile-tech-robotica-platform/retroc-real-time-robot-controller/ (accessed on 22 May 2026).
21. Airtac. HFD Series Compact Air Gripper Catalogue. Product Catalogue/Technical Datasheet. Available online: https://gmsystem.net/wp-content/uploads/2021/06/hfd.pdf (accessed on 14 March 2026).
22. Airtac. 7V Series Solenoid Valve Catalogue. Product Catalogue/Technical Datasheet. Available online: https://us-en.airtac.com/upload/7V-Series-Solenoid-Valve-(5+2-way,-5+3-way)-20260127095422628 6.PDF (accessed on 14 March 2026).
23. VEVOR. TC-20B Airbrush Set User Manual. Product Manual/Technical Documentation. Available online: https://images.thdstatic.com/catalog/pdfImages/c0/c0396713-4f28-5e12-b827-31d777b12647.pdf (accessed on 14 March 2026).
24. Hong, J.H.; Lim, J.H.; Lee, E.; Shin, D. The Workspace Analysis of the Delta Robot Using a Cross-Section Diagram Based on Zero Platform. *Machines* **2024**, *12*, 583. [CrossRef]
25. Ali, H.; Vasques, C.M.A.; Cavadas, A.M.S. Comparative Study of Rigid and Flexible Multibody Dynamics in a 3D-Printed Two-Link Robotic Mechanism. *Eng. Proc.* **2026**, *124*, 112. [CrossRef]
26. Vasques, C.M.A.; Ferreira, J.P.R.; Figueiredo, F.A.V.; Abrantes, J.C.C. On the Electrical Resistivity Measurement Methods and Properties of Conductive 3D-Printing PLA Filaments. *Eng. Proc.* **2025**, *87*, 26. [CrossRef]
27. Vasques, C.M.A.; M. S. Cavadas, A.; Abrantes, J.C.C. Technology overview and investigation of the quality of a 3D-printed maraging steel demonstration part. *Mater. Sci. Addit. Manuf.* **2025**, *4*, 025040002. [CrossRef]

Disclaimer/Publisher's Note: The statements, opinions and data contained in all publications are solely those of the individual author(s) and contributor(s) and not of MDPI and/or the editor(s). MDPI and/or the editor(s) disclaim responsibility for any injury to people or property resulting from any ideas, methods, instructions or products referred to in the content.